論文 95-6-2-3

전파흡수체 정합경계값의 수치계산

(Numerical Computation of Matching Boundary Values of Electromagnetic Wave Absorbers)

김 왕 섭*·김 경 용*·배 규 식**

(Wang-Sup Kim*·Kyung-Yong Kim*·Kyoo-Sik Bae**)

요 약

광대역용 박판 전파흡수체의 설계에는 자성재료가 많이 사용되며, 주로 자성재료 박판의 이면에 금속판을 접착하여 만든다. 이 경우, 6개의 변수를 포함하는 한개의 이론식에 의해 무반사 또는 보다 실용적인 99% 이상의 흡수(20dB 전파감소)가 가능한 전파흡수체의 형상과 재료 및 전자파 상수가 정의된다. 20dB 전파감소에 해당하는 정합 경계값을 계산하기 위하여 Secant법을 적용하였으며, 전파흡수체 설계시 허용 가능한 재료 상수값의 범위를 구하기 위하여 Secant법을 응용한 search algorithm을 개발하였다. 6개의 변수 모두에게 적용할 수 있는 이 수치해석 방법에 의해 최소의 반복 계산으로 정확한 값을 효율적으로 구할 수 있었다.

abstract

The design of broad-band, thin layer electromagnetic wave absorbers usually employs magnetic materials. The common absorber consists of a magnetic material layer bonded to a metal plate at the back. For such structure, a theoretical expression involving six parameters defines the allowable material shape and values of electromagnetic parameters that will produce zero reflection or more practically more than 99% absorption (20dB attenuation). The Secant Method was employed to compute the matching boundary values corresponding to 20dB attenuation. In addition, a search algorithm coupled with the Secant Method was developed to obtain allowable range of material parameters for the design of wave absorbers. These numerical methods applicable to any six parameters effectively yielded accurate solutions in the least iterations.

I. INTRODUCTION

As the use of electromagnetic waves grows with the rapid development of information-cojmmunication technology, "wave pollution" is drawing extensive social concern. Typical examples of

* 한국과학기술연구원 세라믹스재료연구단(Ceramics Processing Lab. Korea Institute of Science and Technology)
** 수원대학교 전자재료공학과(Dept. of Electronic Materials Engineering, The University of Suwon)

the wave pollution are the ghost phenomenon on TV sets and malfunction of electronic equipments due to wave interferance. The most effective measure for removing this problem is the elimination of reflection by absorbing unwanted incident waves. This can be done by cladding buildings with materials capable of absorbing electromagnetic waves. Such wave-absorbing materials are thus required to have large electric and magnetic loss in the frequency range of interest and to be formed into thin plates. Most heavily studied and currently commercialized are magnetic materials such as ferrites[1~4].

The common magnetic wave absorber consists of a magnetic material layer bonded to a metal plate at the back. For such structures, zero reflection (perfect absorption) occurs when the impedance of the structure becomes identical to that of free space. This perfect matching condition is represented by a theoretical equation (Equ. (1)) involving six different variables. This complex equation of the required relationship between the six parameters can only be solved numerically[5, 6]. Approximate solution based upon appropriate assumptions have been often used[1~3]. Recently, Musal et al[5, 6] obtained more accurate solutions numerically by assigning values to four of the six parameters and using a computer-implemented complex-root-finder algorithm. Perfect matching points evaluated in this manner are graphically presented in the form of design chare[1~6]. This graphic aid not only simplifies the design process, but also provides an overall view of the interrelated numerical values of material parameters required to meet the perfect matching condition.

Im practice, however, complying with the perfect matching condition is not only difficult but also unnecessary. 99% absorption (20dB attenuation) is in fact a more practical criterion. But the matching boundary values, corresponding to 99% absorption, cannot be evaluated by the complex-root-finder. Thus, only approximate values obtained by a trial-and-error method have been used[7]. This method is inaccurate and very ineffective, however. In the present study, the Secant Method (SM) was applied to compute matching boundary values. Numerical examples obtained by this method were presented in the form of matching boundary charts. Then, a search algorithm coupled with the SM was developed to obtain allowable minimum and maximum values of given parameters for the design of the electromagnetic wave absorbers.

Ⅱ. THEORETICAL BACKGROUND

For a single-layered absorber attached to a metal plate at the back, the input impedance, Z_{in} normalized by the impedance in free space, Z_o is expressed as

$$Z=\frac{Z_{in}}{Z_o}=\sqrt{\frac{\mu_r}{\varepsilon_r}}\tanh\left[j\frac{2\pi}{c}\sqrt{\mu_r\cdot\varepsilon_r}\cdot f\cdot d\right] \quad (1)$$

where μ_r $(=\mu_r'-j\mu_r'')$, ε_r $(=\varepsilon_r'-j\varepsilon_r'')$, d, c and f represent the relative complex permeability, the permittivity, the thickness of the absorber, the speed of light in vacuum and the frequency of the electromagnetic wave, respectively. When the perfect matching condition is met, the reflection coefficient, Γ of a normally incident plane wave becomes

$$\Gamma=\frac{Z_{in}-Z_o}{Z_{in}+Z_o}=\frac{Z_{in}-Z_o-1}{Z_{in}-Z_o+1}=\frac{Z-1}{Z+1}=0 \quad (2)$$

For the satisfaction of Eq. (2), the normalized input impedance Z must be given by

$$Z = \frac{Z_{in}}{Z_0} = \sqrt{\frac{\mu_r}{\varepsilon_r}} \tanh\left[j \frac{2\pi}{c} \sqrt{\mu_r \cdot \varepsilon_r} \cdot f \cdot d \right] = 1 \quad (3)$$

Any set of six parameters (μ_r', μ_r'', ε_r', ε_r'', d and f) which satisfy Eq. (3) corresponds to a perfect matching point. A typical conventional design chart for the relations between μ_r' and μ_r'' satisfying Eq. (3) on the condition that $\varepsilon_r'' = 0$ is shown in Fig. (1)[7].

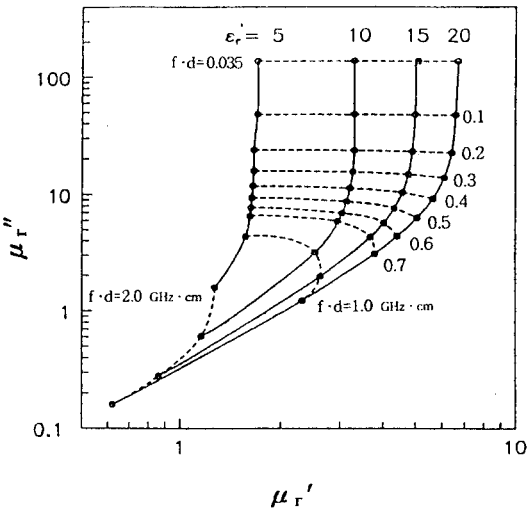

[Fig. 1] Conventional design chart of electromagnetic wave absorber ($\varepsilon_r'' = 0$)[7].

Now, the attenuation value, D is defined as

$$D = -10 \log |\Gamma|^2 = -20 \log |\Gamma| \quad (4)$$

For over 20dB attenuation (less than 1% reflection), D becomes

$$D = -20 \log |\Gamma| > 20 \quad (5)$$

$$|\Gamma| \leq 0.1 \quad (6)$$

At a fixed ε_r and f · d, attenuation behavior is only the function of complex magnetic permeability. Fig 2 represents the attenuation surface as a function of complex permeability at a fixed ε_r (= 20−j · 0) and f · d (= 0.6GHz · cm) values. Each point on the surface corresponds to the attenuation value determined by Eqs. (1) and (4). The matching boundary in which 20dB attenuation occurs is a circular line formed by the cross sectional plane at the 20dB level of the z-axis in Fig. 2. Then, all points on the attenuation surface above this line corresponds to over 20dB attenuation.

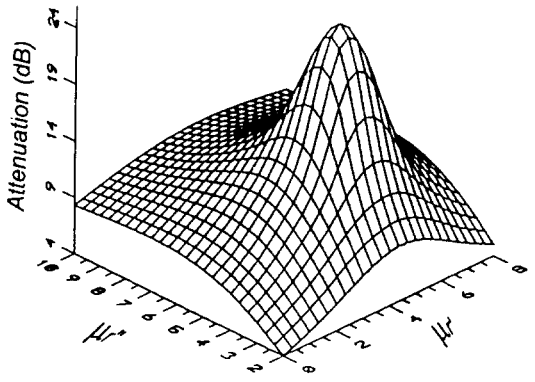

[Fig. 2] Attenuation surface as a function of magnetic complex at a fixed ε_r and f · d values (ε_r = 20−j · 0 and f · d = 0.6GHz · cm).

Ⅲ. NUMERICAL CALCULATION METHOD AND APPLICATION

Eq. (6) can be rewritten as

$$F(f, d, \varepsilon_r', \varepsilon_r'', \mu_r', \mu_r'') = |\Gamma| - 0.1 \leq 0 \quad (7)$$

$$F'(f, d, \varepsilon_r', \varepsilon_r'', \mu_r', \mu_r'') = |\Gamma| - 0.1 = 0 \quad (7)'$$

If numerical values are assinged to any five parameters in Eq. (1), Z now becomes a function of a remaining parameter. When this equation is put into Eq. (2) and then the new equation for Γ is inserted into Eq. (7)', F' becomes a real function of an unknown parameter. For solving the function F', the Secant Method (SM)[8] is employed, since the SM performs effectively with excellant accuracy and convergence rate for a very complicated function such as F'. The use of the SM to find the solution x from two initial guesses X_{-1} and X_0 is illustrated graphically in Fig. 3. Based on $\Delta\mu_r'' = \mu_{r(i)}'' - \mu_{r(i-1)}'' < 10^{-5}$ as a termination test, the SM converged with five-place accuracy in less than 10 iterations.

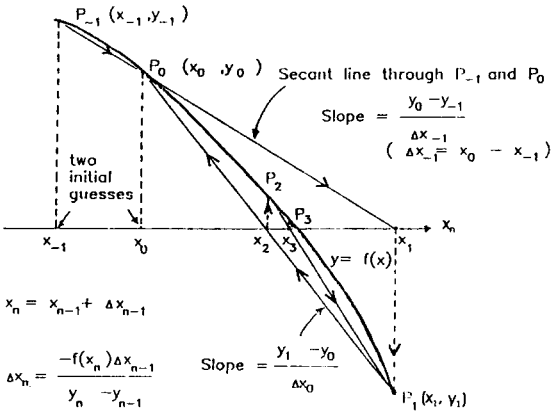

[Fig. 3] Graphical representation of the Secant Method[8]. Starting from two initial guesses, x_{-1} and x_0, iteration is repeated to find the approximate solution x.

Matching boundary values satisfying Eq. (7)' for different ε_r' at the fixed f · d (= 0.6GHz · cm) and ε_r'' (= 0) were obtained by the SM and are presented as a matching boundary chart in Fig. 4. Points located at the center of matching boundaries correspond to perfect matching points and those on boundary circles do to 20dB attenuation. Therefore, any point inside boundaries, not necessarily the perfect matching point, represents allowable μ_r' and μ_r'' values for application as wave absorbers. It is interesting to note that the matching boundary for μ_r' and μ_r'' appears to be a perfect circle. Fig. 4 also shows that the matching boundary as well as the matching point moves to the right and downward with the increasing ε_r' values, as was previously observed[4].

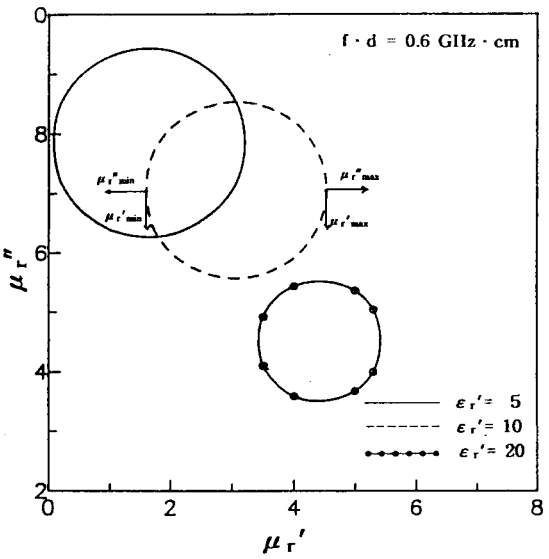

[Fig. 4] Matching boundaries of $|\Gamma| = 0.1$ for different different ε_r' with f · d = 0.6GHz · cm and $\varepsilon_r'' = 0$.

Fig. 5 shows the matching boundary for the case of the f · d values of 0.035GHz · cm and other values kept the same as in Fig. 4. Only the half of oval figure with positive μ_r' values show up in the chart. The values of allowable μ_r'' are larger than those in Fig. 4 by more than an order of magnitude. With increasing ε_r' values, the matching boundary shifts horizontally in the direction

of the increasing μ_r'. Regarding Figs. 4 and 5, it's worth noting that this type of matching boundary chart can be constructed for any two of six parameters by the above numerical method.

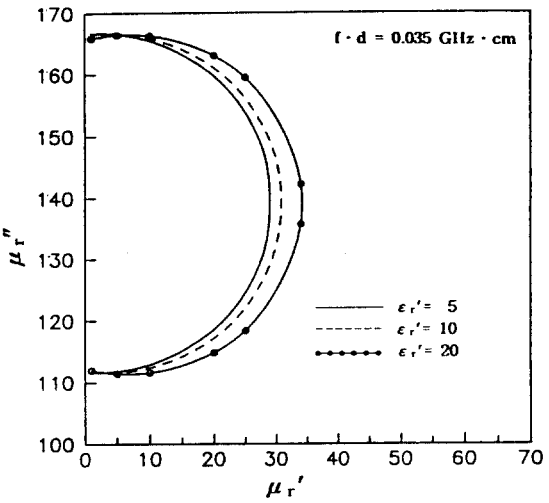

[Fig. 5] Matching boundaries for different different ε_r' with f · d = 0.035GHz · cm and $\varepsilon_r'' = 0$.

Fig. 6 illustrates changes in the matching boundary with increasing f · d values at the fixed ε_r ($= 10 - j \cdot 0$). This figure on the log-log scale shows that allowable μ_r'' ranges shrink as the fd value increases. As the f · d value varies continuously, attenuation surfaces at each f · d value will be overlapped. Then, it is unnecessary to compute values of all points on the matching boundary. Just the maximum and minimum values, as shown in Figs. 7-a and 7-b, are sufficient for the design of wave absorbers. In practice, finding the minimum and maximum values of μ_r ($\mu_{r\,min}'$ and $\mu_{r\,max}'$) and computing values of μ_r'' corresponding to $\mu_{r\,min}'$ and $\mu_{r\,max}'$ ($\mu_{r\,min}''$ and $\mu_{r\,max}''$ as defined in Fig. 4) is more convenient. Then, one can construct a circle from these values and all points inside the circle represent allowable μ_r' and μ_r'' values for the given f · d range (or f range for the fixed d).

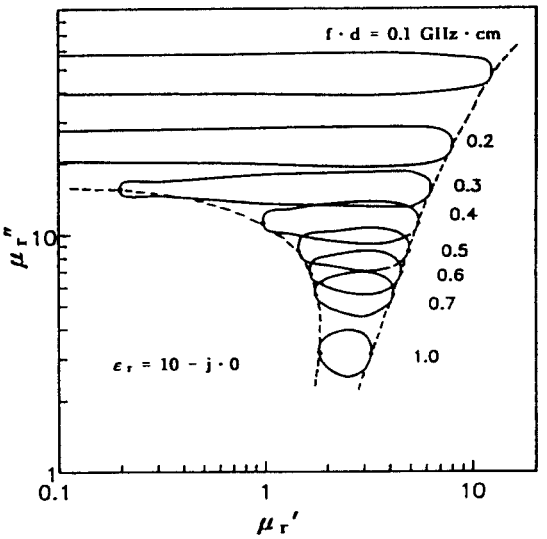

[Fig. 6] Matching boundaries in the log-log scale as a function of f · d values with the fixed ε_r ($= 10 - j \cdot 0$).

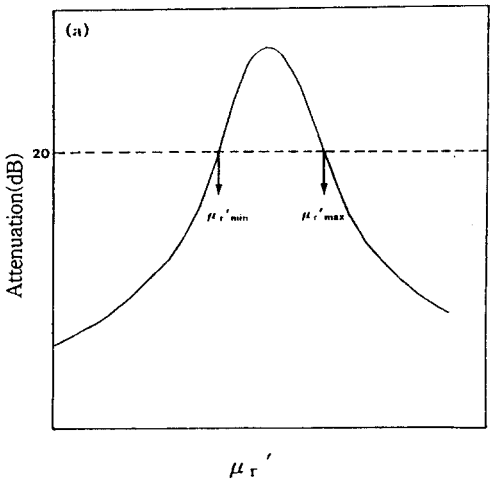

[Fig. 7] Projectional view of the attenuation surface in Fig. 2 from the (a) μ_r' side and (b) μ_r'' side.

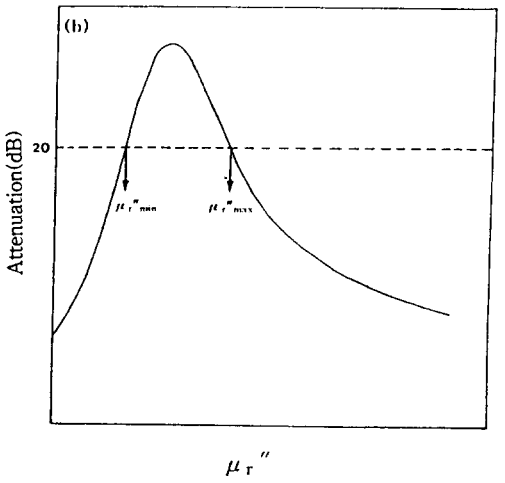

[Fig. 7] Projectional view of the attenuation surface in Fig. 2 from the (a) μ_r' side and (b) μ_r'' side.

A search algorithm coupled with the SM was constructed to find the maximum or minimum values of a parameter. A flow-chart to find the minimum μ_r' value for given f, d, ε_r' and ε_r'' values is shown in Fig. 8. Starting from an initial value (usually "0"), the μ_r' values were asymptotically selected and repeatedy substituted into Eqs, (1), (2) and (7)'. Whether the chosen μ_r' is the solution of Eq. (7) was determined by the SM at each iteration. The increament of μ_r' between successive iterations less than 10^{-5} was chosen as a termination test. This iterative algorithm exhibited rapid convergence to the minimum value within 9 iterations at most. A similar algorithm starting from a large initial value (i.e. "50") yielded the maximum value.

The minimum ($\mu_{r\,min}'$, $\mu_{r\,min}''$) and maximum ($\mu_{r\,max}'$, $\mu_{r\,max}''$) values of μ_r' and μ_r'' were computed for various f · d values at the fixed ε_r (= 10−j · 0) by the above algorithm and displayed in Fig. 9, which is in fact nothing but a modified version of

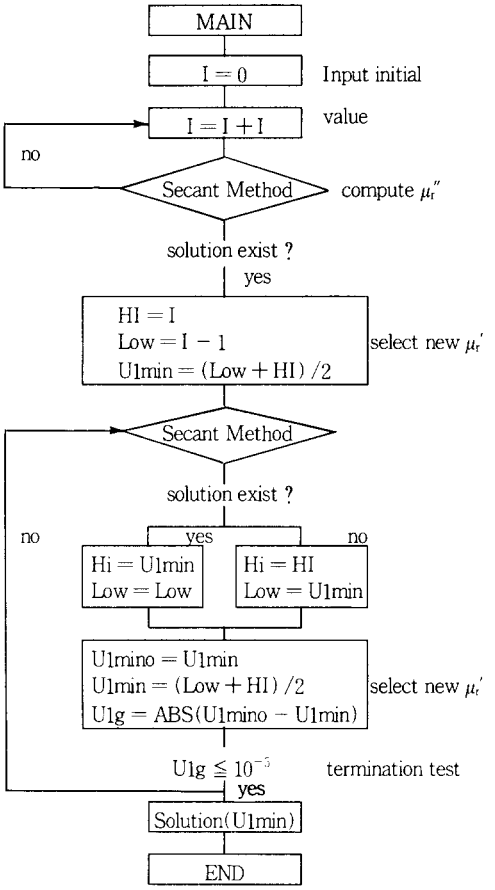

[Fig. 8] A flow-chart consisting of a search algorithm and the Secant Method to find the minimum μ_r'' values.

Fig. 6. The $\mu_{r\,min}''$ and $\mu_{r\,max}''$ show identical values, as expected from the observation that the matching boundary forms a perfect circle (Fig. 4), and decrease with increasing f · d values. In the case of μ_r', $\mu_{r\,max}'$ decreases and $\mu_{r\,min}'$ increases as the f · d value increases. This means that the allowable μ_r' and μ_r'' range decreases with increasing f · d values.

With the f · d (= 0.035GHz · cm) and ε_r'' (= 0) values fixed, the $\mu_{r\,min}'$, $\mu_{r\,max}'$, $\mu_{r\,min}''$ and $\mu_{r\,max}''$ values

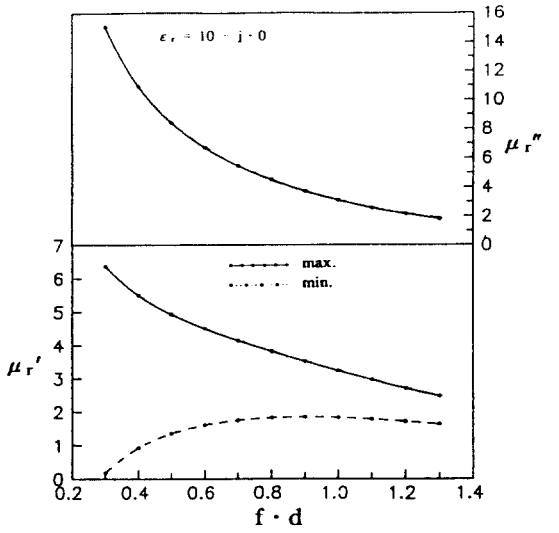

[Fig. 9] The maximum and minimum values of μ_r' and μ_r'' as function of f · d values with the fixed ε_r (= 10−j · 0).

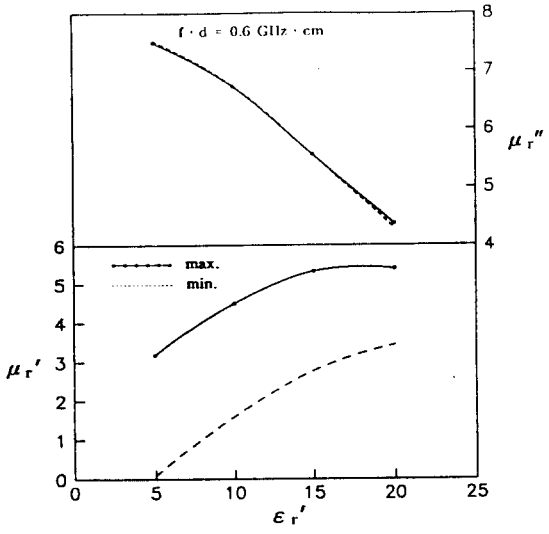

[Fig. 10] The maximum and minimum values of μ_r' and μ_r'' as function of ε_r' values with the f · d = 0.035GHz · cm and $\varepsilon_r'' = 0$.

were computed as a function of ε_r'. The result in Fig. 10 shows that $\mu_r''_{min}$ and $\mu_r''_{max}$ decrease with increasing ε_r' values. In the case of μ_r', both values increase, but the difference between them becomes smaller, as the ε_r' value increases. Therefore, increase in ε_r' results in the reduction of allowable μ_r' and μ_r'' range.

Fig. 11 illustrates changes in the matching boundary as a function of ε_r'' at the fixed f · d (= 0.6 GHz · cm) and ε_r' (= 10) values. Contrary to the case of f · d and ε_r', variations in ε_r'' increases $\mu_r'_{min}$, $\mu_r'_{max}$, $\mu_r''_{min}$ and $\mu_r''_{max}$ altogether. In addition, the difference between the maximum and minimum values grows larger with increasing ε_r'', resulting in the narrower allowable μ_r' and μ_r'' range.

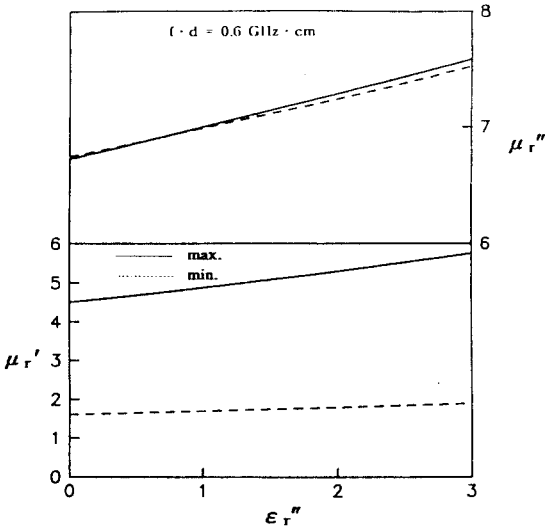

[Fig. 11] The maximum and minimum values of μ_r' and μ_r'' as function of ε_r'' values with the f · d = 0.6GHz · cm and ε_r = 10.

Ⅳ. CONCLUSIONS

In this study, the Secant Method was applied to compute the matching boundary values that correspond to 20dB attenuation. In addition, a search algorithm coupled with the Secant Method

was developed to obtain the allowable minimum and maximum values of given parameters for the design of electromagnetic wave absorbers based on 20dB attenuation. The advantage of these approaches was applicability to any of six parameters and fast convergence to accurate solutions.

These numerical methods were applied to the computation of μ_r' and μ_r''. The matching boundary was shown to develope into a full circle of which size decreased, as the f · d value increased. The minimum and maximum values of μ_r' and μ_r'' were computed as a function of f · d ε_r' and ε_r'' values respectively. The allowable range decreased with increasing f · d and ε_r' while it expanded with increasing ε_r''.

V. REPERENCES

1. Y. Naito and K. Suetake, "Application of Ferrite to Electromagnetic Wave Absorber and Its Characteristics," IEEE Trans. MTT-19(1), 85 (1971)
2. Y. Naito, *Electromagnetic Wave Absorbers*, New OHM Co., Japan, 85 (1987)
3. K. Ishino and Y. Narumiya, "Development of Magnetic Ferrites: Control and Application of Losses," Am. Ceram, Bull., 66, 1469 (1987)
4. E. C. Snelling, *Soft Ferrite - Properties and Applications*, 2nd ed., Butterworths, London, 37(1988)
5. H. M. Musal, Jr and H. T. Hahn, "Thin-Layer Electromagnetic Absorber Design," IEEE Trans. Magnetics-25, 3851 (1989)
6. H. M. Musal, Jr and D. C. Smith, "Universal Design Chart for Specular Absorbers," IEEE Trans. Magnetics-26, 1462 (1990)
7. K. Y. Kim, W. S. Kim and S. Y. Hong, "A Study on a Method to Design an Electromagnetic Wave Absorber with an Attenuation over 20dB," J. Kor. Phys. Soc., 24 (6), 456 (1991)
8. M. J. Maron, *Numerical Analysis: A Practical Approach*, Macmillan Pub. Co. Inc., N. Y. 53 (1982)